Carbohydrate Research 344 (2009) 127–133

Contents lists available at ScienceDirect

Carbohydrate Research

journal homepage: www.elsevier.com/locate/carres

# Comparison of thermochemistry of aspartame (artificial sweetener) and glucose

Mohammad Rashidian, Alireza Fattahi *

*Department of Chemistry, Sharif University of Technology, PO Box 11365-9516, Tehran, Iran*

ARTICLE INFO

*Article history:*
Received 27 November 2007
Received in revised form 25 August 2008
Accepted 1 September 2008
Available online 26 September 2008

*Keywords:*
Aspartame
Glucose
Metal ion affinity
Anion affinity
DFT calculations

ABSTRACT

We have compared the gas phase thermochemical properties of aspartame (artificial sweetener) and α- and β-glucose. These parameters include metal ion affinities with $Li^+$-, $Na^+$-, $K^+$-, $Mg^{+2}$-, $Ca^{+2}$-, $Fe^{+2}$-, $Zn^{+2}$-ions, and chloride ion affinity by using DFT calculations. For example, for aspartame, the affinity values for the above described metal ions are, respectively, 86.5, 63.2, 44.2, 255.4, 178.4, 235.4, and 300.4, and for β-glucose are 65.2, 47.3 32.9, 212.9, 140.2, 190.1, and 250.0 kcal $mol^{-1}$, respectively. The study shows differences between the intrinsic chemistry of aspartame and glucose.



## 1. Introduction

Aspartame (*N*-L-aspartyl-L-phenylalanine-1-methylester) (see Scheme 1), a low-calorie sweetener obtained by synthesis from two amino acids, L-phenylalanine and L-aspartic acid, is very widely used in foods, soft drinks, and dietary products.[1] About 16,000 tons of aspartame is produced for worldwide consumption each year.

Aspartame's attractiveness as a sweetener comes from the fact that it is approximately 180 times sweeter than sugar in typical concentrations without the high energy value of sugar. While aspartame, like other peptides, has a caloric value of 4 kcal (17 kJ) per gram, the quantity of aspartame needed to produce a sweet taste is so small that its caloric contribution is negligible, which makes it a popular sweetener for those trying to avoid calories from sugar.

Clinical studies showed that usage of excess aspartame may cause various health problems such as headaches, migraines,[2] and memory loss.[1]

Although it is relatively stable in its dry form, pH, temperature, and time are very important factors affecting its stability in solution.[3] Below pH 3, aspartame is unstable and hydrolyzes to produce aspartylphenylalanine and above pH 6, it cyclizes to form 5-benzyl-3,6-dioxo-2-piperazine acetic acid.[4] Both forms result in a loss of sweetness.[3] It cannot be used in products that are baked or fried due to disintegration upon exposure to high temperatures.[3]

The investigation of the complexes of metal ions which are vital for biological systems is important because it can clarify clinical results. As apparent from the formula, aspartame can also exist as a ligand by means of carboxylate and amino groups for the crucial metal ions in biological processes.[5] The studies on aspartame and its metal complexes in solution phase have attracted increasing interest in recent years.[1,5–15]

The involvement of metal ion–saccharide interactions in key biological processes, such as the binding of metal ions to cell walls[16] and $Na^+$-glucose transmembrane transport[17], has created interest in the gas phase (i.e., intrinsic) chemical properties of the metal ion complexes of saccharides. Unfortunately, literature

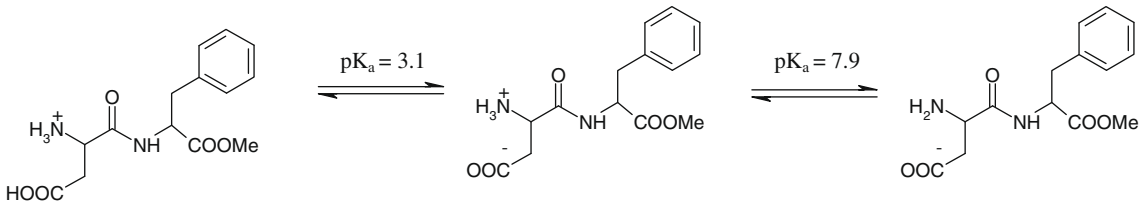


**Scheme 1.** Molecular structure and p$K_a$ values of aspartame.[1]

* Corresponding author.
*E-mail address:* fattahi@sharif.edu (A. Fattahi).

0008-6215/$ - see front matter © 2008 Elsevier Ltd. All rights reserved.
doi:10.1016/j.carres.2008.09.020

about the intrinsic chemistry of aspartame and glucose in the solvent-free environments (i.e., gas phase) has remained scarce. To the best of our knowledge, a detailed comparison between intrinsic chemistry of aspartame and glucose has never been determined at a level of theory as high as B3LYP/6-31+G(d,p).

In the present study, the thermochemistry and structures of the $Li^+$, $Na^+$, $K^+$, $Mg^{2+}$, $Ca^{2+}$, $Fe^{2+}$, $Zn^{2+}$, and $Cl^-$ complexes of α- and β-glucose and aspartame, as well as their gas phase acidities have been examined and compared by density functional theory (DFT) calculations.

## 2. Computation method

Initial search of minima on the potential energy surface for α- and β-glucose, aspartame, and their metal complexes were carried out by MMFF level using SPARTAN software.[18] The most stable conformers were optimized by the density functional (DFT) method using Becke three parameter hybrid exchange and Lee–Yang–Parr correlation (B3LYP)[19,20] employing 6-31+g(d,p) basis set with SPARTAN. This basis set was selected for all calculations as it contains both polarized basis set and diffuse functions. Diffuse functions are particularly important for systems where electrons are relatively far from the nucleus including molecules with lone pairs and anions.[21–23] Similar basis sets were used in the reproduction of metal affinities in a series of studies devoted to the investigation of alkali ion-amino acids or nucleobase interactions at both density functional and ab initio correlated levels.[21,24–26] From these studies, it is possible to conclude that the metal ion affinity (denoted by MIA) values obtained at B3LYP level are generally affected by an average error of about 2–3 kcal $mol^{-1}$ with respect to experimental values.[27]

Complexations energies considered the zero-point vibrational energy (ZPVE), temperature correction to the vibrational enthalpy, (5/2)*RT* for the translational energy of the metal, and the pressure volume work term. Vibrational frequencies were also used at the corresponding level of theory in order to verify that each complex obtained was at an energetically minimum state and not at a transition state.

MIA of α- and β-glucose and aspartame at 298 K is defined as the negative of enthalpy ($-\Delta H^0_{rxn}$) for the gas phase reaction

$$X + M^+ \rightarrow [X - M]^+ \quad (1)$$

where X is α-glucose, β-glucose, or aspartame.Using the standard thermodynamic scheme we can write

$$\Delta H^{298} = \Delta E^{298} + \Delta(PV) \quad (2)$$

$$\mathrm{MIA(X)} = -\Delta H^{298} = -U[X - M^+] + U[X] + U[M^+] + 2.5RT \quad (3)$$

In Eq. 3, *U* is the computed absolute energy and 2.5*RT* is the kinetic energy contribution of $M^+$ at 298 K. The same equations were used to calculate the chloride affinity values of α- and β-glucose, and aspartame. The low spin state of $Fe^{2+}$ was used to calculate the corresponding $Fe^{2+}$ affinity values.

## 3. Result and discussion

### 3.1. Structure and conformation analysis of free molecule

The first step was to identify all of the minima on the conformational potential energy surface for aspartame, its zwitterionic form, glucose and its anionic forms starting from a selection of several low-lying conformations for these dipeptides and carbohydrates with the relative energy in the range of 10 kcal, by using SPARTAN program.

### 3.2. Aspartame (asm)

For aspartame, 100 conformers were found in the range of 10 kcal. The most stable conformer was then optimized by using B3LYP/6-31+g(d,p). The optimized structure is given in Figure 1 from two views to better clarify the structure (Fig. 1a and b).

For the zwitterionic form of aspartame (zw-asm), 45 conformers were found in the range of 10 kcal. The most stable conformer was then optimized using B3LYP 6-31+g(d,p). However, as seen in Figure 1c, the zwitterionic structure was collapsed to nonzwitterionic (nzw) form by transferring a proton from ammonium group to carboxylate group. This rearrangement occurs because transferring a proton leads to neutralization of charges and formation of a new and strong hydrogen bond (1.77 Å). Thus, we can call it a new conformer of asm; however, it should be mentioned that this collapsed structure is not the most stable conformer of asm.

### 3.3. Glucose

As expected, for α- and β-Glc, our calculations show that pyranose structures are the most stable conformers. They are more stable than open conformers and furanose conformers. Therefore, calculations are restricted to pyranose forms.

For α- and β-Glc, 75 and 39 conformers were found in the range of 10 kcal, respectively. The most stable conformers were then optimized using B3LYP/6-31+g(d,p). The optimized structures are shown in Figure 2.

The favored glucose structures predicted computationally contain pyranose rings in chair conformations that permit four or five hydrogen bonds between the hydroxyl groups, as shown in Figure

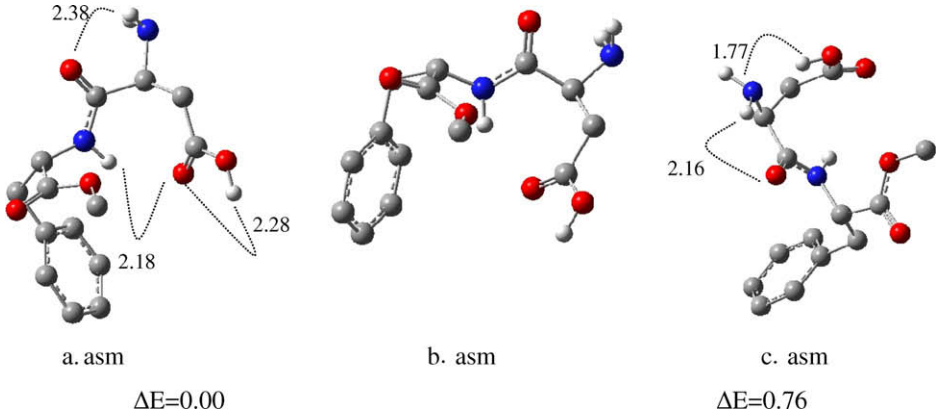


**Figure 1.** The optimized structures of aspartame (**1a** and **1b**, the same) and its collapsed structure of zwitterionic form (**1c**) and their relative energies ( kcal $mol^{-1}$).

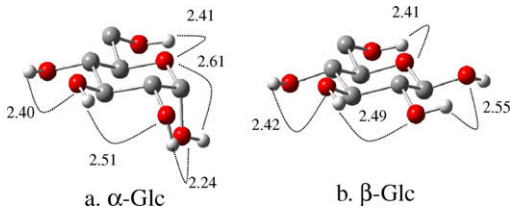


**Figure 2.** Optimized structures of α- and βGlc at B3LYP/6-31+g(d,p).

2. As expected, all OH groups in both α- and β-Glc are in equatorial positions, except for the anomeric OH of α-Glc which is located on the axial position.

### 3.4. Comparison of MIA and $Cl^-$ affinity of aspartame and glucose

Based on DFT calculations, metal ion affinities (MIAs) of asm and α- and β-Glc have been calculated using the following equations:

$$\text{asm} + M^{n+} \rightarrow \text{asm} - M^{n+} - \Delta H^{o}_{rxn} = \text{MIA} \quad (\text{asm}) \qquad (4)$$

$$\text{Glc} + M^{n+} \rightarrow \text{Glc} - M^{n+} - \Delta H^{o}_{rxn} = \text{MIA} \quad (\text{Glc}) \qquad (5)$$

The calculated MIAs are given in Table 1. As seen in Table 1, the MIAs of aspartame are considerably larger than those of glucose. The MIAs of two anomers of glucose (α- and β-glucose) are relatively alike. For instance, the MIAs of β-Glc with $Li^+$, $Na^+$, $Mg^{2+}$, and $Ca^{2+}$ are, respectively, 65.2, 47.3, 212.9, 140.2 kcal $mol^{-1}$. However, the MIAs of aspartame with $Li^+$, $Na^+$, $Mg^{2+}$, and $Ca^{2+}$ are, respectively, 86.5, 63.2, 255.4, and 178.4 kcal $mol^{-1}$. The detailed structural analysis of metal ion complexes of Glc and asm are given in the following sections.

### 3.5. Metal ion complexes of α- and β-Glc

The lowest-energy conformers (LECs) of α- and β-Glc–$M^{n+}$ complexes are given in Figures 3 and 4. For some of the molecules and complexes, two conformers are given to show the influence of hydrogen bonding on the given relative energy ($\Delta E$) of the two conformers.

Neutral saccharides can exist in a large number of pyranose conformations. The preferred pyranoses contain chairs with most substituents in equatorial positions, both in solution[28] and in the gas phase.[29–36] Conformational analysis of glucose rings has shown that the preferred shape is the chair that has all substituent groups in equatorial orientations, the anomeric oxygen will be axial or equatorial as dictated by whether the compound is α- or β-glucose (Figs. 3a, b and 4a, b).

The best coordination of the complexes of saccharides with metal ions (Sac–$M^{n+}$) may, however, be achieved by less stable chair or boat conformers that can more efficiently coordinate the metal ion (Fig. 4g and m). Due to such conformational complexity, it is very difficult to assess the structure of the (Sac–$M^{n+}$) complexes from the experimental data alone. Small changes in the saccharide stereochemistry alter the optimum $M^{n+}$ coordination possible and, therefore, the $M^{n+}$ affinity.[37] Thus, the metal ion affinity is ideally suitable for the distinction of stereoisomeric saccharides. Herein, to obtain more information on the nature of the Glc–$M^{n+}$ bond, the geometries and energies of several Glc–$M^{n+}$ conformers have been interrogated computationally. For instance, as seen in Figures 3 and 4, the structures of α-Glc–$M^{2+}$ and β-Glc–$M^{2+}$ are completely different because of the anomeric OH.

As seen in Figures 3 and 4, the favored Glc–$M^{n+}$ structures predicted computationally are in $^4C_1$ and $^1C_4$ forms or boat conformations that permit tri- or tetradentate–$M^{n+}$ coordination and hydrogen bonds between the hydroxyl groups. In the calculated structures, the pyranose O atom and the hydroxymethyl group generally participate in the $M^{2+}$ binding, in agreement with the experimental trends.[27] These investigations show that the most stable Glc–$M^{n+}$ isomers generally result from charge solvation of $M^{n+}$ by the oxygens (Figs. 3 and 4).

In case of monovalent cations, such as $Li^+$, α- and β-Glc exist as a bidentate chelate (Figs. 3c, f and 4c, f). Four hydrogen bonds exist in each of these complexes and make them more stable. It should be pointed out that the trends in the calculated MIAs of α- and β-Glc are in accord with the hard–soft acid–base concept. The better matched the donor and acceptor, the stronger and bigger are the complexation and MIAs. For instance, the MIAs of β-Glc with $Li^+$, $Na^+$, and $K^+$ are 65.2, 47.3, and 32.9 kcal $mol^{-1}$, respectively. For $Li^+$–Glc complex, the hard–hard electrostatic interactions between $Li^+$ and $O^-$ results in the stronger metal complexation, as compared with $Na^+$–Glc, and $K^+$–Glc complexes (Fig. 6). Interestingly for both α- and β-Glc complexes with $K^+$ (Figs. 3e, f and 4e, f) slight difference is observed in coordination pattern. In both cases, in the most stable one, $K^+$ is coordinated with –O3 and –O4, but in the case of the slightly higher energy forms $K^+$ is coordinated with –O3 and –O2.

In case of divalent cations, such as $Mg^{2+}$, α-Glc ring flips over from the $^4C_1$ to the $^1C_4$ conformation. The hydroxymethyl and other hydroxyl groups, except anomeric one, go to axial positions (see Fig. 3g and m). Thus, α-Glc exists as a tridentate chelator. As seen, the presence of one hydrogen bond also causes the complex of α-Glc with divalent cations to be more stable. But, for divalent cations such as $Mg^{2+}$, $Ca^{2+}$, $Fe^{2+}$, and $Zn^{2+}$, it is surprising that the chair form of β-Glc changes to skew form for better solvation

**Table 1**
Metal ion affinities (MIAs) of α-, βGlc, and asm in kcal $mol^{-1}$

| System | $M^{n+}$ | MIA |
|---|---|---|
| α-Glc | $Li^+$ | 66.0 |
| | $Na^+$ | 48.1 |
| | $K^+$ | 33.5 |
| | $Mg^{2+}$ | 198.3 |
| | $Ca^{2+}$ | 129.8 |
| | $Fe^{2+}$ | 173.6 |
| | $Zn^{2+}$ | 237.0 |
| β-Glc | $Li^+$ | 65.2 |
| | $Na^+$ | 47.3 |
| | $K^+$ | 32.9 |
| | $Mg^{2+}$ | 212.9 |
| | $Ca^{2+}$ | 140.2 |
| | $Fe^{2+}$ | 190.1 |
| | $Zn^{2+}$ | 250.0 |
| Asm | $Li^+$ | 86.5 |
| | $Na^+$ | 63.2 |
| | $K^+$ | 44.2 |
| | $Mg^{2+}$ | 255.4 |
| | $Ca^{2+}$ | 178.4 |
| | $Fe^{2+}$ | 235.4 |
| | $Zn^{2+}$ | 300.4 |

The basis set for all calculations is 6-31+g(d,p).

**Table 2**
Chloride Affinity of α-, βGlc, and asm in kcal $mol^{-1}$

| System | Complex | Chloride ion affinity |
|---|---|---|
| α-Glc | $Cl^-$–α-Glc | 31.0 |
| β-Glc | $Cl^-$–β-Glc | 32.4 |
| asm | $Cl^-$–asm | 30.3 |

The basis set for all calculations is 6-31+g(d,p).

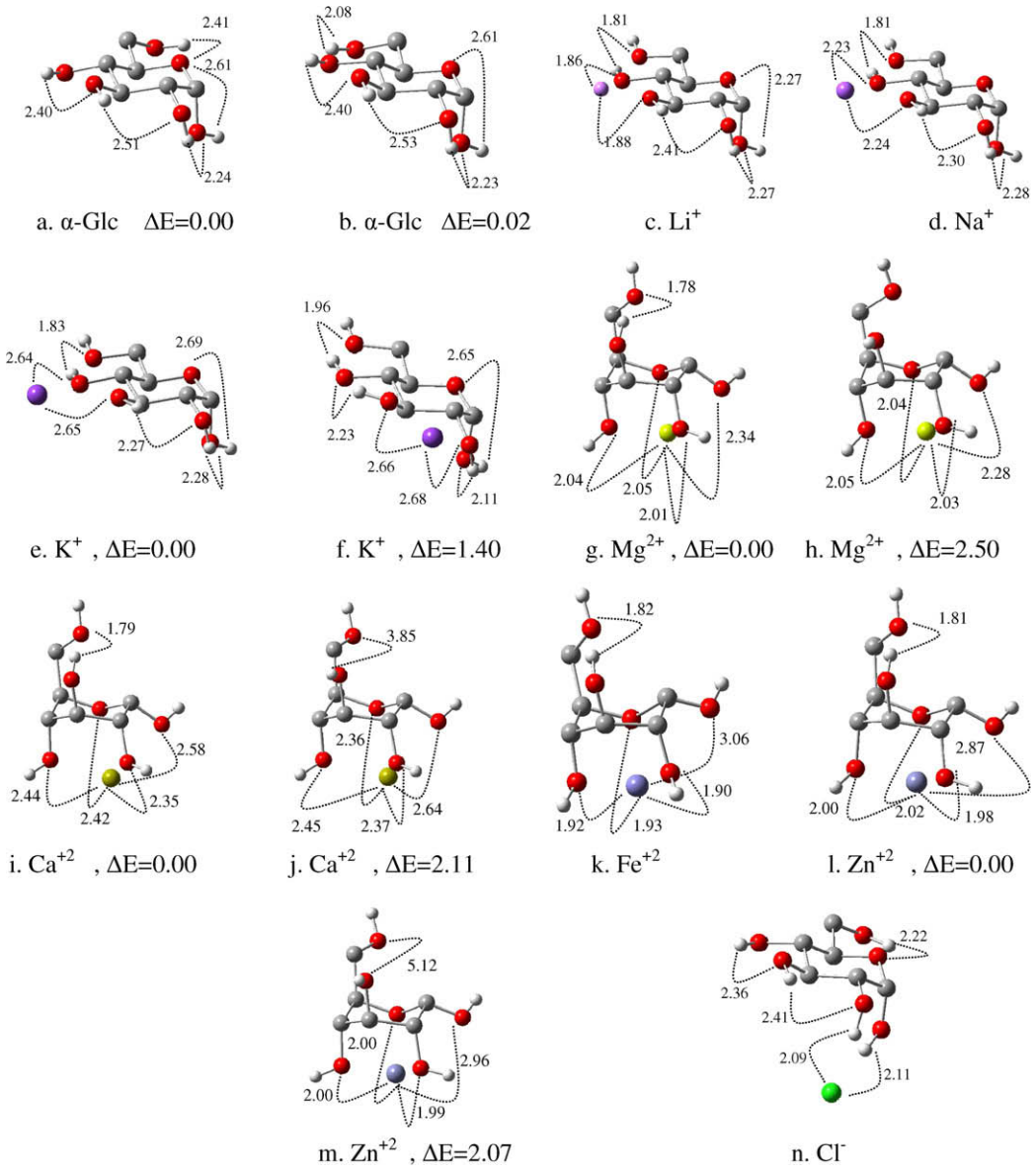


**Figure 3.** B3LYP/6-31+g(d,p) LECs for α-Glc, $Cl^-$–α-Glc and $M^{n+}$–α-Glc. Δ*E*s are in kcal $mol^{-1}$.

(Fig. 4g and m). It is worthwhile to mention that all OH groups in the chair form of β-Glc are in equatorial positions; so flipping to the skew conformer can result in destabilization. However, β-Glc–$M^{2+}$ prefers the skew conformer because it makes a tetradentate-complex in the skew conformer. For example, compare the complexes of α-Glc–$Mg^{+2}$ with β-Glc–$Mg^{+2}$ and α-Glc–$Fe^{+2}$ with β-Glc–$Fe^{+2}$ in Figures 3g, k and 4g, k. As clearly shown, for divalent cations, α-Glc exists as a tridentate ligand, whereas β-Glc exists as a tetradentate ligand.

As a representative and important biological anion, we explored the chloride complexation of asm and Glc. As shown in Figures 3n, 4n, and 5l, in each of these complexes, chloride anion binds to the molecule through two HBs. This results in a similar chloride affinity for asm, α- and βGlc (Table 2).

### 3.6. Metal ion complexes of asm

As seen in Figure 5, for asm–$M^{n+}$ the most stable conformers usually result from charge solvation of $M^{n+}$ by three carbonyl oxygens of carboxylic, ester, and amide groups. In case of $M^{2+}$-complexes side-chain phenyl group will also help coordination of $M^{2+}$.

In case of monovalent cations, such as $Li^+$, aspartame exists as a tridentate chelator (Fig. 5c). The presence of two hydrogen bonds (2.14 and 2.30 Å) in these monovalent complexes makes them more stable. As seen in Table 1, the MIAs for the complexes of asm with $Li^+$, $Na^+$, and $K^+$ are 86.5, 63.2, and 44.2 kcal $mol^{-1}$, respectively. Similar to the trends for α- and βGlc, these trends in the MIAs of asm agree with the hard–soft acid–base concept (Fig. 6).

However, in case of divalent cations, such as $Mg^{2+}$, aspartame changes its structure completely in that phenyl ring has interaction with $M^{2+}$ and thus asm becomes folded. Therefore, asm can be considered as a tetradentate chelator for $M^{2+}$ (Fig. 5e).

As seen in Figure 5e and g, an electrostatic interaction exists between the divalent ions and the phenyl group of aspartame. These cation–π interactions present in a variety of proteins binding cationic substrates represent an area of growing interest.[4,38–40] Many interesting examples of metal ion–aromatic side chain

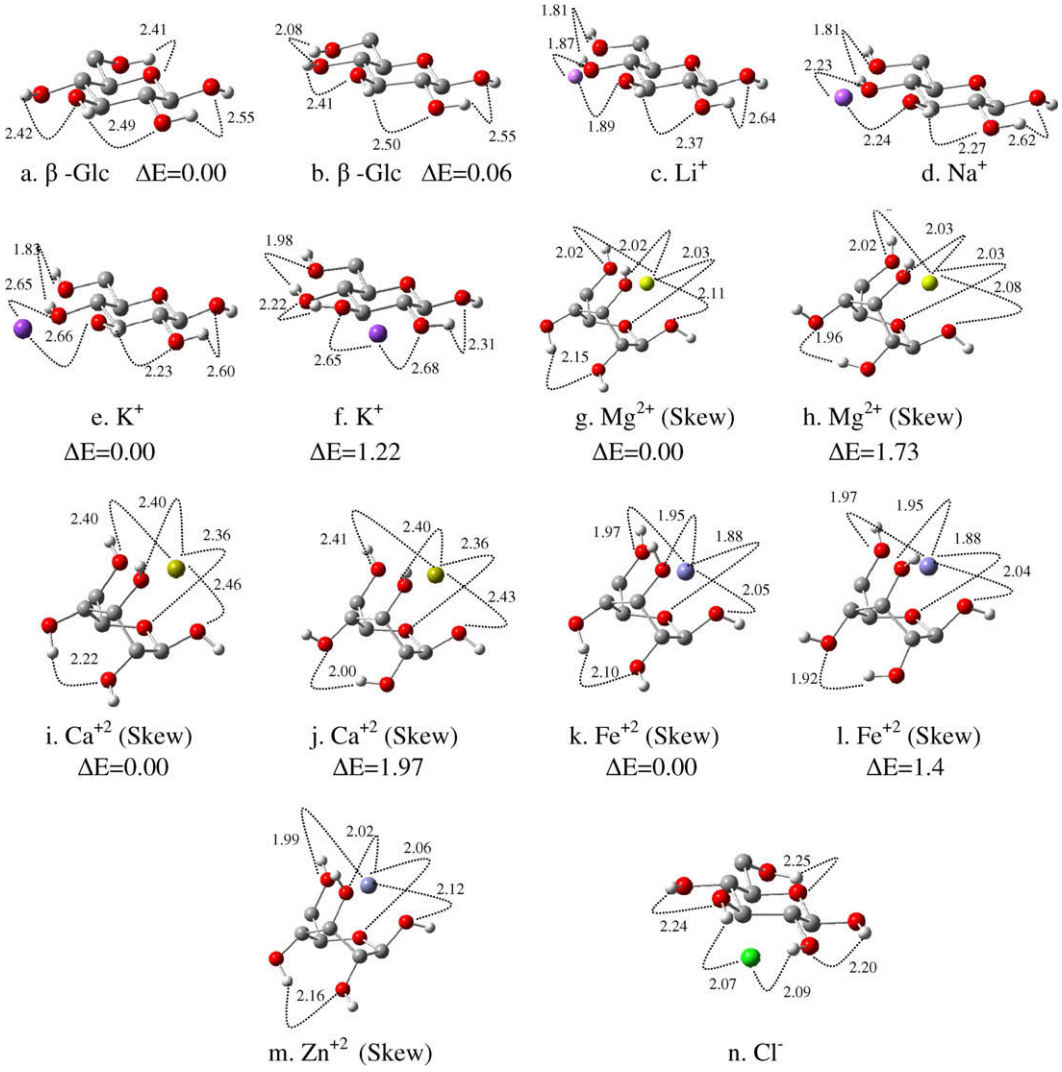


**Figure 4.** B3LYP LECs for β-Glc, $Cl^{-}$–β-Glc and $M^{n+}$–β-Glc, relative energies ($\Delta E$ in kcal $mol^{-1}$) are given in 298 K.

**Table 3**
Relative energies of nzw–asm–$M^{2+}$ and zw–asm–$M^{2+}$ (for the same metals) at 298 K, in kcal $mol^{-1}$

| System | $M^{n+}$ | Relative energy |
|---|---|---|
| Asm | $Mg^{2+}$ | 0.00 |
| | $Zn^{2+}$ | 0.00 |
| Zw–asm | $Mg^{2+}$ | −0.54 |
| | $Zn^{2+}$ | −3.30 |

The basis set for all calculation levels is 6-31+g(d,p).

interactions have been found in crystal structures, in solutions, and in the gas phase. For example, in the crystals of bis(tyrosinato) copper(II),[41] bis(tyrosinato) palladium(II),[42] and (Gly–Leu–Tyr) Cu(II)[43] the metal ion and the aromatic ring are located within bonding distance. In solution, planar complexes of $Ni^{2+}$ and $Pd^{2+}$ with amino acids, di- and tripeptides have a dramatic increase in population of the conformation that has a side chain situated over a coordinated metal ion if the chelating molecule contains an aromatic side chain.[44] In the gas phase, collision-induced dissociation (CID) of divalent metal–oligopeptide complexes leads to predominant loss of fragments that do not contain aromatic side chains,[45,46] suggesting strong participation of the aromatic groups in metal–ion binding. Such effects are particularly strong for transition metal ions where orbital interactions almost certainly play an important role,[38] to the extent that Ma and Dougherty[39] suggested not considering transition metal–aromatics as noncovalent complexes. Not many examples of cation–π effects can be found for ions with which one would expect predominantly electrostatic interactions (like alkali and alkaline-earth ions). Hu et al.[45] found that $Ca^{2+}$, $Sr^{2+}$, and $Ba^{2+}$ complexes of tri- and tetrapeptides containing aromatic amino acid residues tend not to lose these residues during CID, displaying a behavior similar to the transition metal–ion complexes, although not as profoundly.

It is well known that most of amino acids exist in a nonzwitterionic form in gas phase. For aspartame, as discussed in Section 1, our results indicate that its nonzwitterionic form is more stable than its zwitterionic form. However, it is worth to mention that aspartame in its zwitterionic form makes stronger attractions with divalent cations ($Mg^{2+}$ and $Zn^{2+}$) than its nonzwitterionic form. Based on calculation results, the complex of zw–asm–$Zn^{2+}$ is not collapsed any more and that is 3.30 kcal $mol^{-1}$ more stable than nzw–asm–$Zn^{2+}$ complex (Table 3). This accordingly suggests the existence of stronger interactions between zwitterionic form of asm and divalent

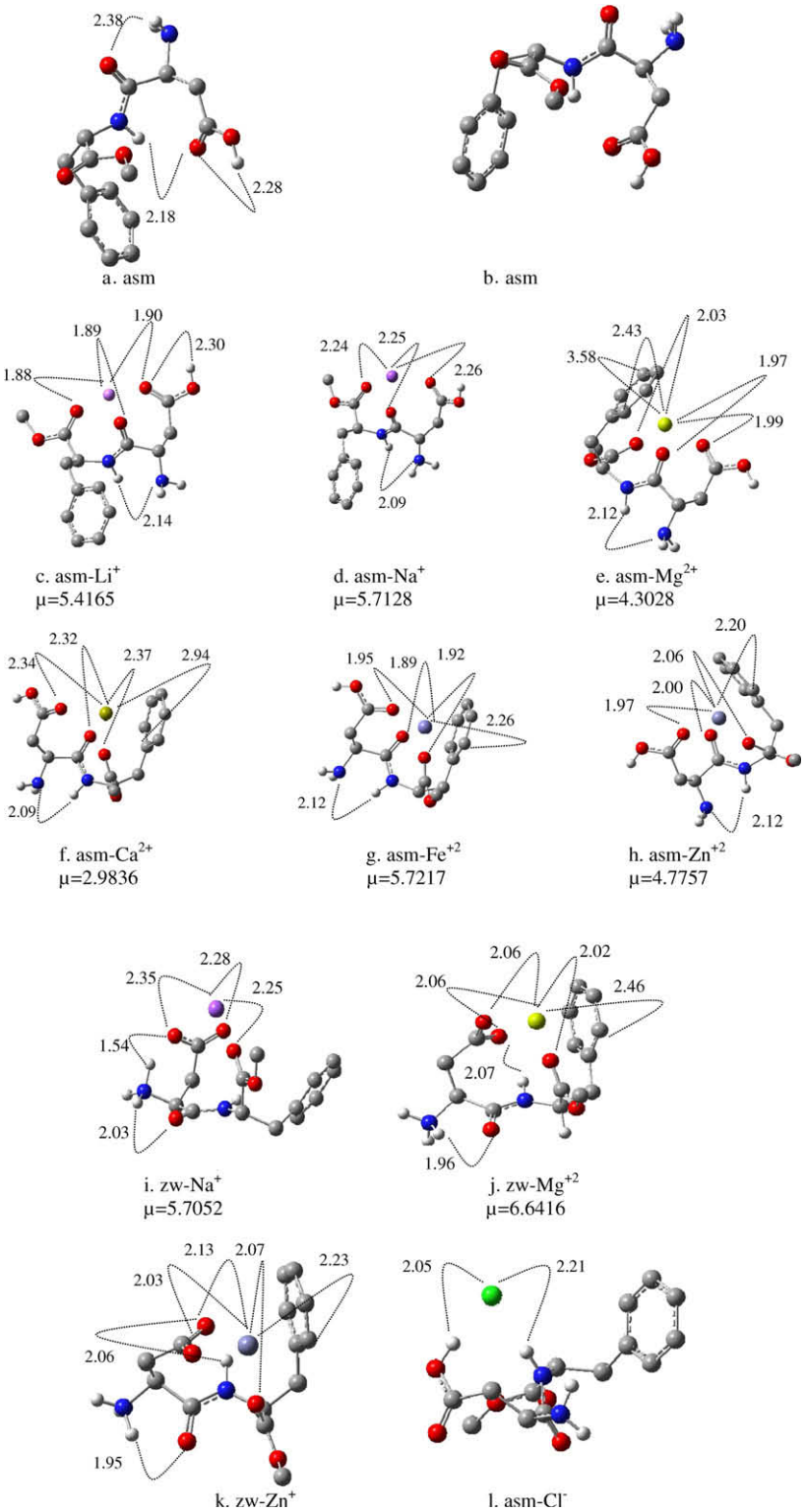


**Figure 5.** B3LYP LECs for asm, $Cl^-$–asm and $M^{n+}$–asm.

cations. This can be explained by the fact that carboxylate is a strong bidentate ligand, and thus can interact with $M^{2+}$ and make the zwitterionic complex sufficiently more stable to exist. The ammonium group also makes a new hydrogen bond which makes it more stable (Fig. 5j). As illustrated in Figure 5j and e, zw form can have two hydrogen bonds instead of one in nzw form.

## 4. Conclusion

The current study indicates that aspartame as artificial sweetener and glucose as natural sugar have different intrinsic thermochemical properties. The results show that MIA of aspartame is larger than that of glucose, and glucose and aspartame indicate similar chloride affinity.

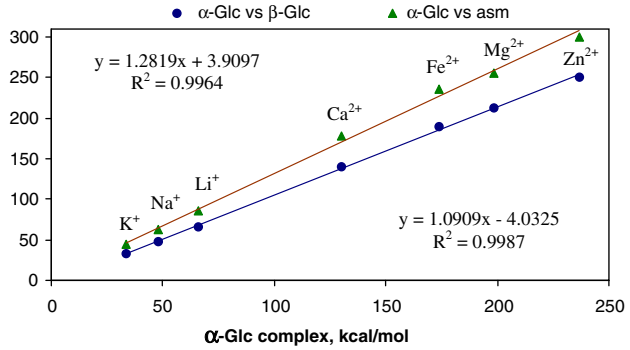


**Figure 6.** MIAs of α-Glc versus βGlc and aspartame.

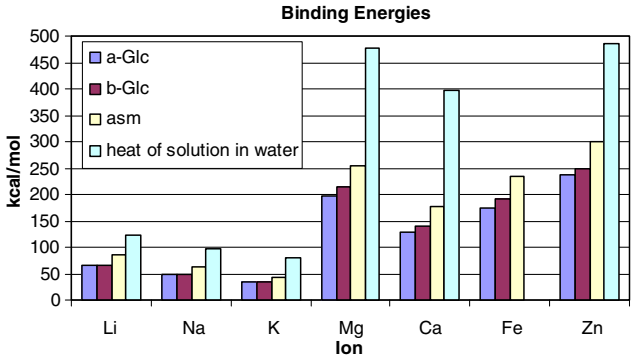


**Figure 7.** MIAs of aspartame, α- and βGlc and heat of solution of ions in water.[47]

In view of the above differences (Figs. 6 and 7) and the fact that aspartame is proved to be a strong chelate even in aqueous solution,[1] we are planning to start studies on the biochemical properties of aspartame as artificial sweetener before complete metabolism.

## Acknowledgments

We wish to thank Dr. M. Gharagozlou for helpful discussions. Support from Sharif University of Technology is gratefully acknowledged.

## References

1. Akir, S. C.. *Carbohydr. Res.* **2003**, *338*, 1217–1222.
2. Newman, L. C.; Lipton, R. B. *Headache* **2001**, *41*, 899–901.
3. Gibbs, B. F. *J. Chromatogr., A* **1996**, *725*, 372–377.
4. Dougherty, D. A. *Science* **1996**, *271*, 163–168.
5. Kholeif, S.; Anderegg, G. *Inorg. Chim. Acta* **1997**, *257*, 225–230.
6. Makar, G. K. R.; Touche, M. L. D.; Williams, D. R. *J. Chem. Soc., Dalton Trans.* **1976**, 1016–1018.
7. May, P. M.; Linder, P. W.; Williams, D. R. *J. Chem. Soc., Dalton Trans.* **1977**, 588–595.
8. Goerss, A. L.; Wagner, G. C.; Hill, W. L. *Life Sci.* **2000**, *67*, 1325–1329.
9. Manion, C. V.; Howard, J.; Ogle, B.; Parkhurst, J.; Edmundson, A. *Clin. Pharmacol. Ther.* **2001**, *69*, 346–355.
10. Giron, D. *Pharm. Sci. Technol. To.* **1998**, *1*, 191–199.
11. Kim, S. K.; Jung, M. Y.; Kim, S. Y. *Food Chem.* **1997**, *59*, 273–278.
12. Sabah, S.; Scriba, G. K. E. *J. Pharm. Biomed. Anal.* **1998**, *16*, 1089–1096.
13. Gozel, P.; Gassman, E.; Michelsen, H.; Zare, R. N. *Anal. Chem.* **1987**, *59*, 44–49.
14. Spiers, P. A.; Sabounjian, L.; Reiner, A.; Myers, D. K.; Wurtman, J.; Schomer, D. L. *Am. J. Clin. Nutr.* **1998**, *68*, 531–537.
15. Galletti, G. C.; Chiavari, G.; Bocchini, P. *J. Anal. Appl. Pyrol.* **1995**, *32*, 137–151.
16. Burger, K. *Biocoordination Chemistry: Coordination Equilibria in Biological Active Systems*; Ellis Horwood: New York, 1990.
17. Cowan, J. A. *Inorganic Biochemistry: An Introduction*; VCH: New York, 1993.
18. SPARTAN 04; *Wavefunction*, Inc.; Irvine, CA.
19. Becke, A. D. *J. Chem. Phys.* **1993**, *98*, 5642–5648.
20. Lee, C.; Yang, W.; Parr, R. G. *Phys. Rev. B* **1988**, *37*, 785–789.
21. Marino, T.; Russo, N.; Toscano, M. *J. Inorg. Biochem.* **2000**, *79*, 179–185.
22. Hoyau, S.; Ohanessian, G. *Chem. Eur. J.* **1998**, *4*, 1561–1569.
23. Bertran, J.; Rodriguez-Santiago, L.; Sodupe, M. *J. Phys. Chem. B* **1999**, *103*, 2310–2317.
24. Marino, T.; Russo, N.; Toscano, M. *J. Phys. Chem. B* **2003**, *107*, 2588–2594.
25. Marino, T.; Russo, N.; Toscano, M. *J. Inorg. Chem.* **2001**, *40*, 6439–6443.
26. Marino, T.; Russo, N.; Toscano, M.; Grand, A. *J. Phys. Chem. B* **2006**, *110*, 24666–24673.
27. Toscano, M.; Russo, N.; Grand, A. *J. Am. Chem. Soc.* **2001**, *123*, 10272–10279.
28. (a) Angyal, S. J. *Adv. Carbohydr. Chem. Biochem.* **1984**, *42*, 15–68; (b) El Khadem, H. S. *Carbohydrate Chemistry: Monosaccharides and Their Oligomers*; Academic: San Diego, 1988.
29. Barrows, S. E.; Storer, J. W.; Cramer, C. J.; French, A. D.; Truhlar, D. G. *J. Comput. Chem.* **1998**, *19*, 1111–1129.
30. Polavarapu, P. L.; Ewig, C. S. *J. Comput. Chem.* **1992**, *13*, 1255–1261.
31. Jebber, K. A.; Zhang, K.; Cassady, C. J.; Chung-Phillps, A. *J. Am. Chem. Soc.* **1996**, *118*, 10515–10524.
32. Brown, J. W.; Wladkowski, B. D. *J. Am. Chem. Soc.* **1996**, *118*, 1190–1193.
33. Ha, S.; Gao, J.; Tidor, B.; Brady, J. W.; Karplus, M. *J. Am. Chem. Soc.* **1991**, *113*, 1553–1557.
34. Van Eijck, B. P.; Hooft, R. W. W.; Kroon, J. *J. Phys. Chem.* **1993**, *97*, 12093–12099.
35. Cramer, C. J.; Truhlar, D. G. *J. Am. Chem. Soc.* **1993**, *115*, 5745–5753.
36. Cerda, B. A.; Wesdemiotis, C., unpublished results.
37. Cerda, B. A.; Wesdemiotis, C. *Int. J. Mass Spectrom.* **1999**, *189*, 189–204.
38. Ma, J. C.; Dougherty, D. A. *Chem. Rev.* **1997**, *97*, 1303–1324.
39. Caldwell, J. W.; Kollman, P. A. *J. Am. Chem. Soc.* **1995**, *117*, 4177–4178.
40. Minoux, H.; Chipot, C. *J. Am. Chem. Soc.* **1999**, *121*, 10366–10367.
41. Van Der Helm, D.; Tatsch, C. E. *Acta Crystallogr., Sect. B* **1972**, *28*, 2307–2312.
42. Sarat, M.; Jesowski, M.; Kozlowski, H. *Inorg. Chim. Acta* **1979**, *37*, L511.
43. Franks, W. A.; Van Der Helm, D. *Acta Crystallogr., Sect. B* **1971**, *27*, 1299–1310.
44. Vestues, P. I.; Martin, R. B. *J. Am. Chem. Soc.* **1980**, *102*, 7906–7909.
45. Hu, P.; Sorensen, C.; Gross, M. L. *J. Am. Soc. Mass Spectrom.* **1995**, *6*, 1079–1090.
46. Cerda, B. A.; Cornett, L.; Wesdemiotis, C. *Int. J. Mass Spectrom.* **1999**, *193*, 205–226.
47. Anslyn, E. V.; Dougherty, D. *A. Modern Physical Organic Chemistry*; University Science Books, Sausalito: California, 2006. p 167.